

HiSST: 4th International Conference on High-Speed Vehicle Science Technology

22 -26 September 2025, Tours, France



Impact damage on Ceramic Matrix Composites – Behaviour and handling

Dr Guillaume Fischer¹

Abstract

Because high velocity means high temperature on airframes, ceramic matrix composites (CMCs) are often seen as very suitable materials for such application. Depending on the family of CMC, they can retain their mechanical properties up to 1000°C (typically oxide-based composites), 1600°C (carbon and silicon carbide-based composites) or even above 2000°C (ultra high temperature ceramic-based materials). The term thermostructural was originally designed for materials with such properties. Airframe parts are intrinsically exposed to any external environment of the vehicle. Having these parts made out of CMCs raises the question of their behaviour regarding these environments. Acceptable effects of the environments are usually defined in a specification. Among the various effects that can be found in a specification, mechanical impact is a concern for CMCs. Low velocity impact damage can be associated to a falling tool, hail or projected pebbles. Coupons from an oxide-based CMCs were tested with different impact energies at low velocity. Similarly to organic matrix composites (OMCs) different regimes can be identified, based on the rate of absorbed energy. The extent of the internal damage, such as delamination, was also determined and correlated to the damage regime. Gathering the data that can be found in the scientific literature on low velocity impact of CMCs, as well as the results from the aforementioned tests a comparison was drawn with OMCs. Common principles were interestingly raised but strong differences remained. The transitions between the damage regimes is lower by one order of magnitude for CMCs than OMCs

Keywords: Ceramic Matrix Composites, Low velocity impact, Mechanical properties, Structural health

Nomenclature

E_{per} – Perforation threshold

Latin h – Thickness a – Shortest or free edge length K - Stiffness

b – Edge length other than a Greek

D – Flexural rigidity α – Shape factor E – Young modulus ν – Poisson ratio

E_{pen} – Penetration threshold

1. Impact cases for structural materials

Impacts are commonly sorted out according to the impactor velocity. Low velocity impacts typically correspond to falling objects on a structure such as a tool during the manufacturing phase of the component or hail during its operational phase. The range of impact speed in this case is typically from 1 to 10 m/s. A second category, which can be called kinetic or ballistic impacts, involves weapon projectiles and pyrotechnic shocks. The range of impact speed is around 100 to 1000 m/s. Above 1000 m/s hypervelocity impacts can be found. Impact of fragments in space can be seen as an illustration.

Speed is not the only parameter which describes an impact. The corresponding energy is also a very useful value to determine. In the case of low velocity and kinetic impacts, it is common to use the kinetic energy of an impactor to perform a test. The relationship between the impact velocity and the

¹ MBDA France

energy is then simply given by the kinetic energy formula. The mass impactor, its shape and its size also count as parameters of interest of the impact.

When it comes to structural composite materials, impact damage has been extensively studied, however the large majority of the literature on this topic deals with polymer-based composites. Even if the components of CMCs are intrinsically different from those of OMCs, these studies provide a useful framework. This work proposes to discuss and illustrate how this framework can be applied to ceramic matrix composites. It will mainly deal with low velocity impacts and to some extent with examples of kinetic impacts.

2. Low velocity impact of an oxide/oxide composite

Oxide/oxide flat panels were manufactured to obtain samples of 150×100 mm² with an average thickness of 2.3 mm. All the plies were oriented at 0 and 90°, leading to a balanced orthotropic laminate.

The samples were impacted using a method inspired from AITM1-0010, which is similar to other standards such as ASTM D7136 or ISO 18352. The samples were clamped on four points on a metallic frame. A 16 mm diameter hemispherical-head steel impactor was dropped from an adjustable height to introduce an impact with a predefined energy at the geometrical centre of the sample. The load and displacement of the impactor were measured all along the impact duration. Integrating the load according to the displacement provides the energy (Fig 1).

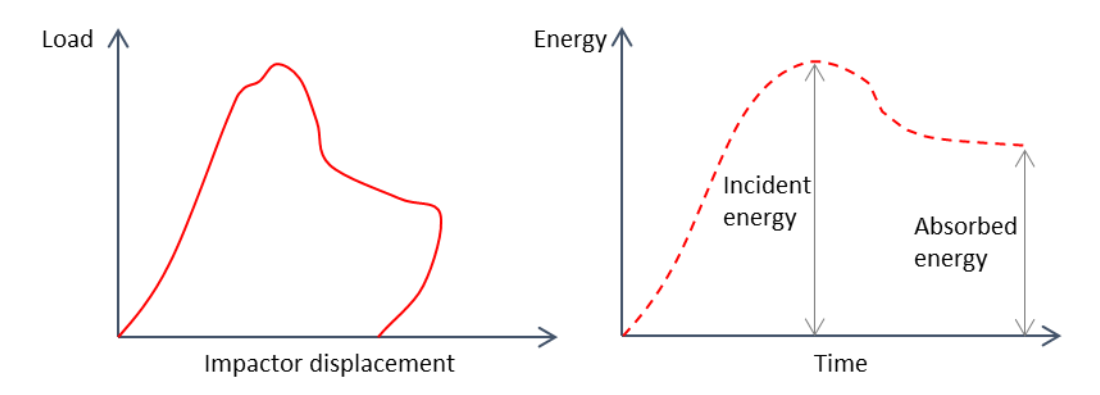


Fig 1. Shape of the load/displacement and energy/time curves

Theoretical impact energy were calculated using the weight potential energy of the impactor (1.215 kg). Targeted energies of impact were 1, 2, 2.5, 3, 4 and 5 J. However due to the lack of accuracy of the test device in this range of small energies, they have been corrected using the energy/time curve in each test (see Fig 1). In this work, the incident energy is defined as the energy effectively transferred to the sample. It can be different from the energy absorbed by the sample.

Pictures of the damaged samples are shown in Table 1. Damage on the back side is visible starting with the lowest impact energy. It consists in cracks with broken fibres, suggesting the failure of some bundles in tension. In the meantime, potential damage is not always visible on the front side. At 3.6 J, a significant damage is observed on both sides. On the front side, a cavity is formed with the hemispherical shape of the impactor. On the back side, large out-of-plane displacement of the plies, cross-shaped teared, can be observed.

The load/displacement curves for the samples impacted at different energies are given on Fig 2. A change of shape can be observed between 2.6 J and 3.6 J. Up to 2.6 J curves are looping back after reaching a maximum load. At 3.6 J and above, the load decrease is accompanied with an increase of the displacement. This change of regime correspond to the significant increase of the damage described previously.

Both regimes have been well identified, originally on OMCs. In the first regime, some of the energy is returned to the impactor which bounces back. The decrease of the displacement on the load/displacement curves correspond to the impactor moving backward. This regime is often called rebound regime. In the second regime observed here, the impactor does not bounce back, which is visible with no decrease of the displacement. It is usually called penetration regime. A third regime

exists, in which the impactor completely goes through the sample. It is called perforation regime but has not been observed here.

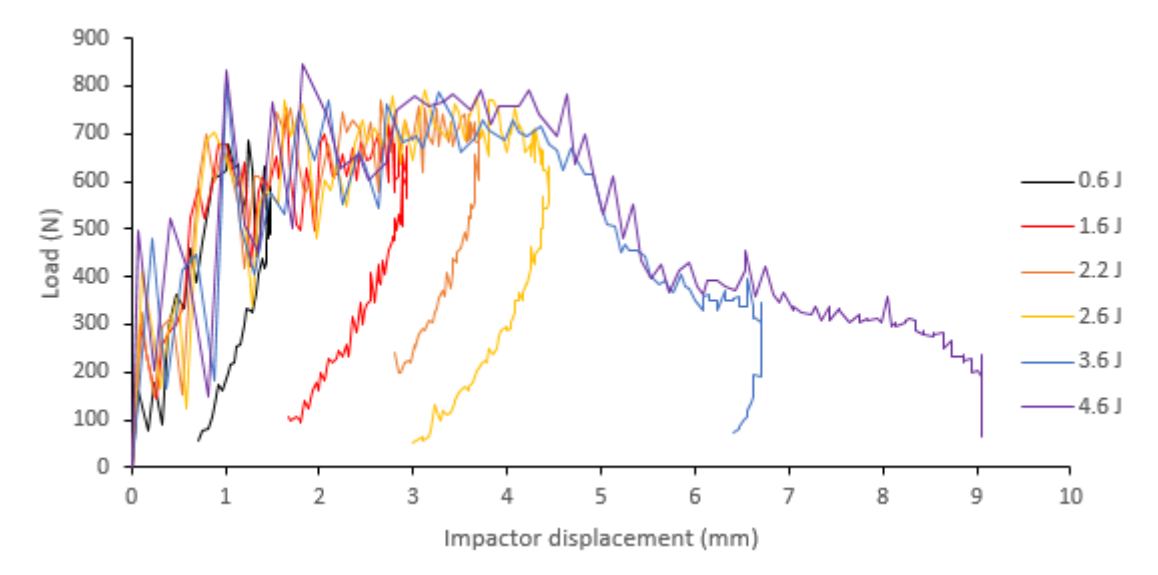


Fig 2. Load/displacement curves during the impacts

Calculating the absorbed energy using the full integral of the load displacement curves, a comparison can be made with the incident energy (Fig 3). The rebound regime can be identified by an absorbed energy lower than the incident energy, the difference corresponding to the energy returned to the impactor. The equality between absorbed and incident energies is characteristic of the penetration regime, indicating a full transfer from the impactor to the sample. In the perforation regime, the absorbed energy would have been again inferior to the incident energy, the difference corresponding to the remaining kinetic energy of the perforating impactor.

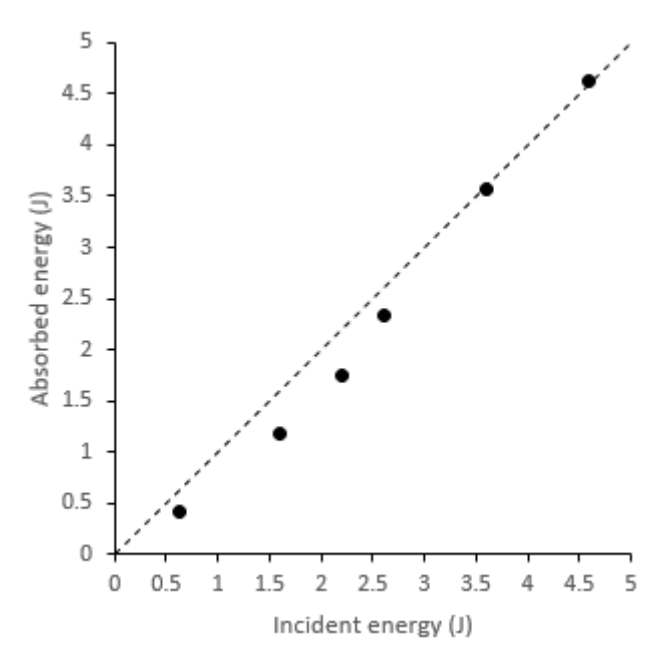


Fig 3. Comparison of the incident energy with the absorbed energy

According to this analysis, the penetration threshold, between the rebound and penetration regimes, for these samples is located close to 3.6 J. The load/displacement curve on Fig 2 at this energy shows a slight decrease of the displacement at the end of the test, indicating a very small rebound.

Front side **Incident energy Back side** 0.6 J 1.6 J 2.2 J 2.6 J 3.6 J 4.6 J

Table 1. Pictures of the samples after impact tests at different energies

The extent of the damage for each sample was investigated with Fourier-transformed infrared (IR) thermography. An example of the resulting pictures is given on Fig 4. It can be seen that the damaged area, indicated here by a dark halo, is much wider than the apparent damaged surface. This suggests that most of the damaging results in delamination between the composite plies. The shape of the damaged area is roughly a diamond but it can also be described as two two-lobed areas oriented along the main directions of a cross.

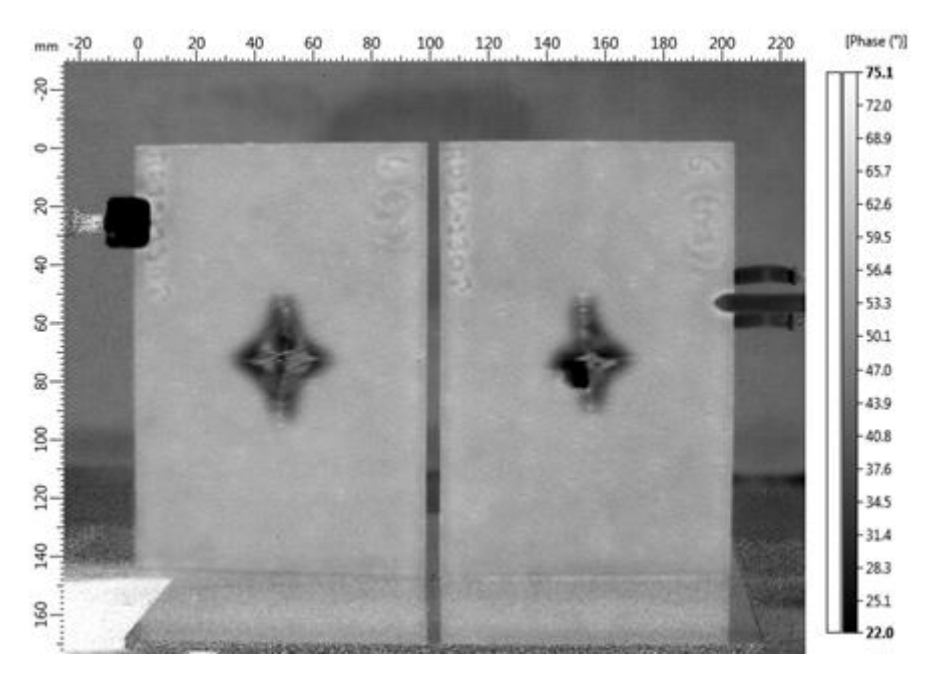


Fig 4. IR thermography of samples impacted at 2.6 J (left) and 2.2 J (right)

IR thermography cannot easily locate the delamination according to the position through the thickness of the laminate. The Fourier-transformed treatment provides indications about this positioning, however the exact identification of the delaminated area for each ply is complex if not impossible in some cases. A convenient analysis is to consider the projected damaged area visible on the thermography pictures. In this case, only the largest area measured was considered among all the pictures for a sample. The hypothesis is made that it corresponds to the area in which delamination is found. Fig 5 displays the evolution of the projected damaged area with the incident energy. The damaged area increases until it seems to reach a plateau, starting between 2.5 to 3.5 J. It is worth noting that the penetration threshold, previously determined around to 3.6 J, is close to the onset of the plateau. Several phenomena are then observed from this point: A change of regime in which the energy is fully absorbed by the sample, a saturation of the delaminated area and a significant increase of the visible damage with a strong out-of-plane strain of the material on the back side. This suggests that the penetration regime can be characterized by the abundance of fibre breakage and plies tearing which add up to the delamination already existing in the rebound regime.

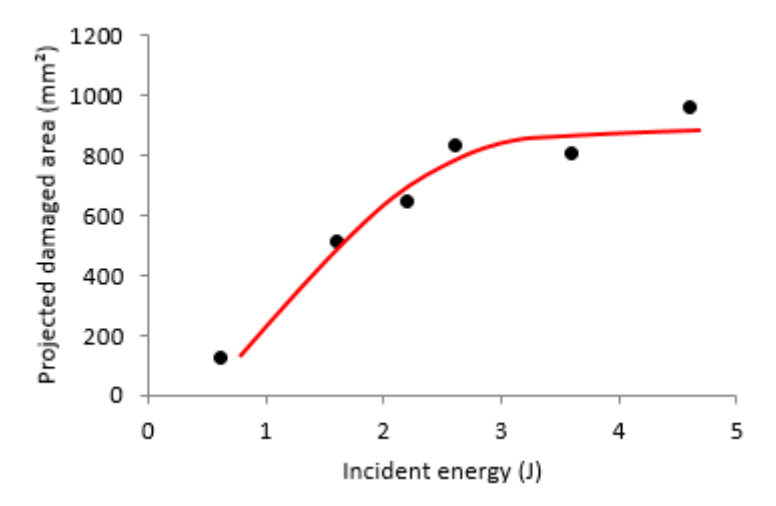


Fig 5. Projected damaged area of impacted samples

3. Literature data for impact tests on Ceramic Matrix Composites

This part proposes to review the previous results in the scope of other existing studies involving impact damage of CMCs. Experimental parameters and results were gathered from scientific papers which shown similarities with the previous study. Some pieces of information are explicit in these articles, others were calculated or estimated. For instance the kinetic energy relationship allows to determine one parameter among the incident energy, the mass and the velocity of the impactor. The incident and absorbed energies can also be determined with curves involving load, displacement and time. If not explicitly stated by the authors, the regime can be estimated with the impacted samples pictures (for the perforation regime) and comparing the incident and absorbed energies (rebound or penetration regimes). The incident energy values were calculated as much as possible to check if they are in agreement with the values indicated by the authors. In the rare cases of disagreement, the calculated value was preferred. The projected damaged area can be directly obtained from the data in the studies. In some cases the damage size estimation is made by the authors at several locations such as front or back side and inside the sample through IR thermography. The maximum is always chosen as a projection. Damage size or surface estimation have sometimes been made based on the pictures of the samples after impact. The database resulting from this analysis is given in appendix.

The gathered data is evenly shared between three families of CMCs, Ox/Ox, C/SiC and SiC/SiC that are respectively obtained with alumina, carbon and silicon carbide fibre reinforcements. Most of them are based on woven fabrics.

The range of impact velocities covers both the low velocity and kinetic domains defined previously. It is worth noting that a quasi-static indentation study was included as a very low velocity case [1]. If various impactor sizes and masses can be found, they all have a spherical or hemispherical shape.

Despite not having parameters determined exactly in the same manner, the aim of this comparison is to draw trends about the behaviour of CMCs when subjected to impact. These trends will be discussed in the next parts.

4. Global analysis of the impact behaviour of Ceramic Matrix Composites

A global trend can be observed by simply plotting the projected damaged area and the incident energy for all the experiments for which this information is available. The result is shown on Fig 6. Two main populations can be identified. The first one displays a strong increase of the projected damaged area with the incident energy, which remains on the lower end of the range, typically inferior to 7 J. The second one shows a projected damaged area that stays low despite exploring the full range of energies up to 22 J. These two populations correlate quite well with the impact velocity as shown on Fig 6. With few exceptions, impacts with a velocity higher than 80 m/s are found in the second population. Impacts with a velocity lower than 20 m/s all belong to the first population.

Very interestingly, these two populations sorted according to the impact velocity correspond to the low velocity and kinetic impact cases described in the first part. This reflects how the velocity, more than the energy, is a determining factor to describe the impact behaviour. With the approximation that the projected damaged area mainly reflects the extent of the composite delamination, it can be stated that low velocity impacts promote delamination over a wide area as an energy dissipating mechanism. Considering the studies that deal with kinetic impacts, several mechanisms can be suggested to explain the lower extent of delamination. In most of the relevant articles, the expulsion of material on the back side, on an area wider than the impactor cross section, is either clearly identified [2] or suggested by the pictures and cross-cut showing the damages [3-5]. Part of incident energy has to be converted into damage but also kinetic energy transferred to the ejected material. In any case, material expulsion requires fibre breakage, which is commonly observed for the kinetic impacts studies [2-6]. The change of damage typology with the impact velocity has to be related with the mechanical response of the specimen regarding the impact duration and the time for mechanical waves to reach the edges of the sample. Increasing the velocity reduces the time of impact causing the response to be dominated by dynamics effects (vibration) [7]. This is also supported by the fact that the quasi-static study [1] fits well in the group of low velocity impacts [8-10].

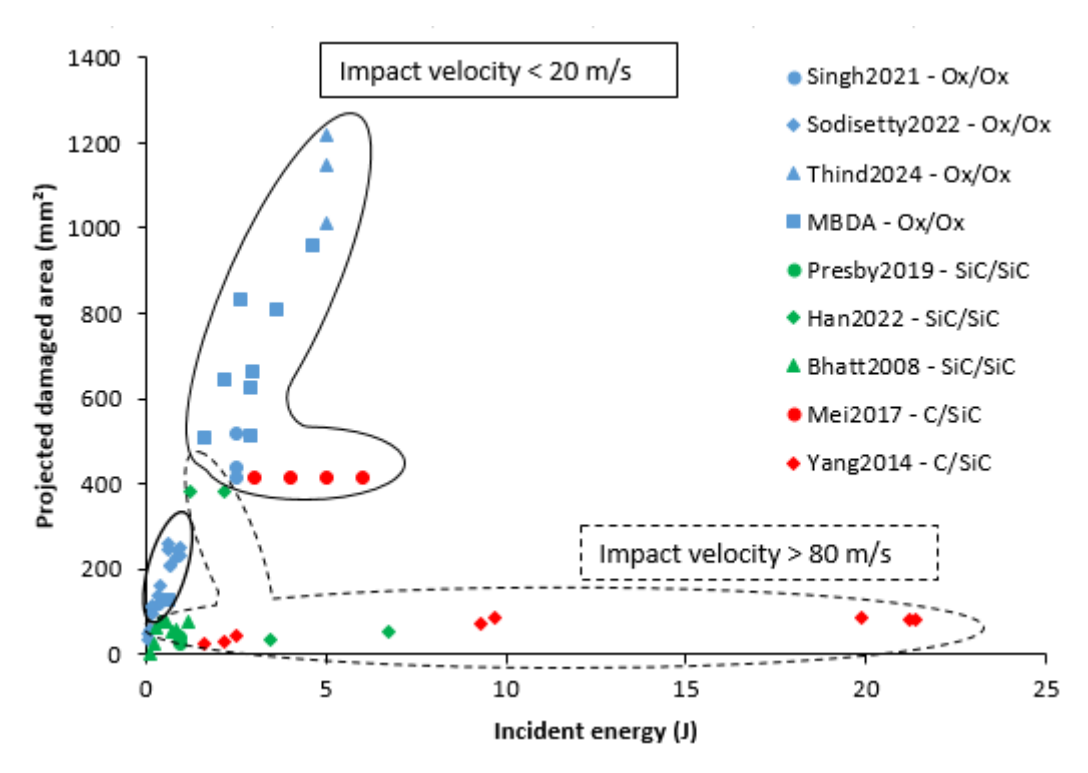


Fig 6. Mapping of the projected damaged are with the incident energy

The data from the literature also provides information on the impact regime for each sample. It can be used to estimate the location of the penetration and perforation energy thresholds, respectively E_{pen} and E_{per} . These thresholds can be discussed according to numerous parameters. In the following part, the data for the low velocity impacts only have been considered.

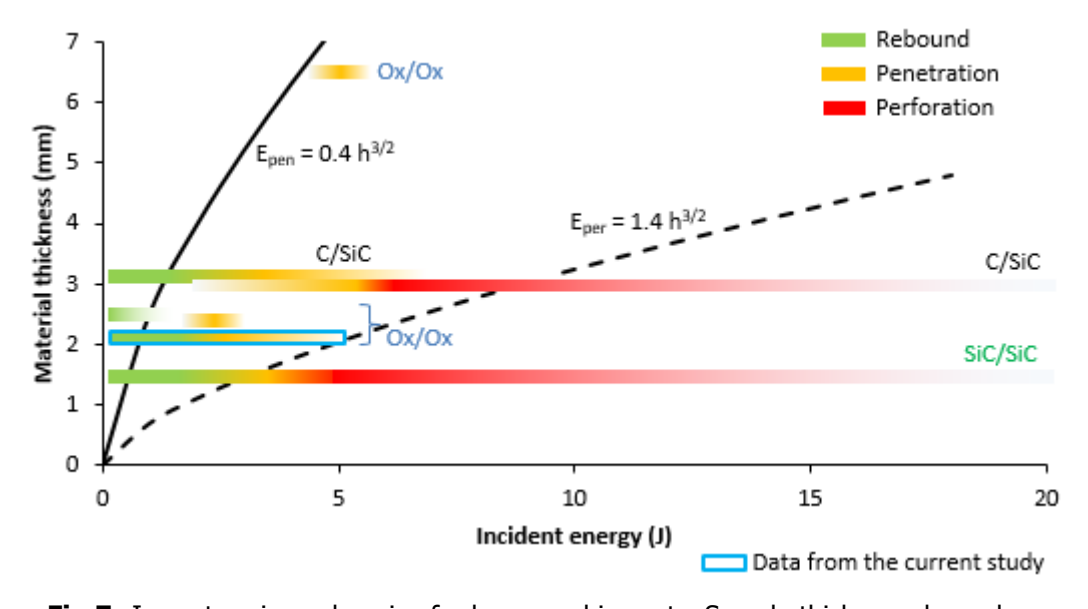


Fig 7. Impact regimes domains for low speed impacts. Sample thickness dependency

None of the selected studies includes tests on a single material with several thicknesses. Combining the observations from the different articles offers the opportunity to get a global trend. The estimated domains for the three impact regimes regarding the thickness of the samples is shown on Fig 7. Since the influence of the thickness on the impact domains has not been found in the selected studies on CMCs, a principle applied to OMCs [11] has been used here. In this procedure, the thickness dependency of the energy thresholds is found to be a simple power law with an exponent close to 1.5. Such model curves have been represented on Fig 7, h being the sample thickness. The factors have been arbitrarily defined to place the curves in a relatively good agreement with the domains estimated

HiSST-2025-XXXX Page | 7 Impact damage on Ceramic Matrix Composites – Behaviour and handling Copyright © 2025 by author(s) for each study. Not all the domains limits fit the curves but the thickness still provide a rough global trend. The sample thickness is obviously not the only parameter involved in the determination of the domains.

The sample stiffness can be estimated using the plate theory [12]. The flexural rigidity D is defined by Eq. 1, where E is the Young modulus of the material, h the sample thickness and ν the Poisson ratio of the material. This formula is not rigorously applicable to an orthotropic material for which E and ν vary according to the direction.

$$D = \frac{Eh^3}{12(1-\nu^2)} \tag{1}$$

The stiffness depends on the sample shape and boundary conditions. Two main cases were identified in the studies under consideration, rectangular (or square) samples with four clamped edges [8, 1, 9, 13, 14] and rectangular samples with two opposite clamped edges [10]. The stiffness K for the former case is given by Eq. 2 and for the latter by Eq. 3, where a is either the shortest edge length (for Eq. 2) or the free edge length (Eq. 3), b is the other edge length and α is a parameter that depends on the b/a ratio which can be found in [12]. These calculations rely on the plate behaviour with a small deflection. As a result only the initial contact, prior to damaging, is considered for these calculations.

$$K = \frac{1}{\alpha} \frac{D}{a^2} \tag{2}$$

$$K = \frac{192Db}{a^3} \tag{3}$$

The resulting stiffness is given for each considered study on Fig 8. The Poisson ratio was fixed at 0.25 for all the materials, a variation between 0.2 and 0.3 is not expected to change the global trend. Unfortunately, no study involving a SiC/SiC composite provided enough data to be used here. The regime domains can be identified, suggesting that the stiffness is a good indicator of the behaviour.

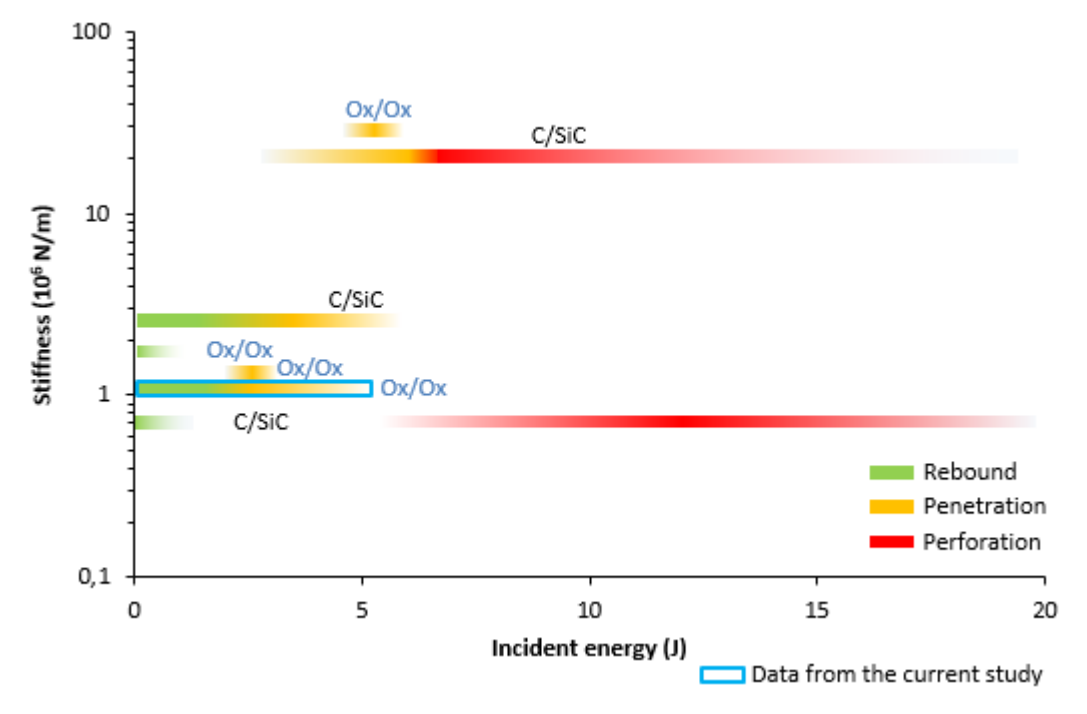


Fig 8. Impact regimes domains for low speed impacts. Stiffness dependency

Going further on the prediction of the impact regime of a CMC sample would require a better knowledge of the damage processes to define the proportion of the incident energy which is dissipated through this process.

5. Potential guidelines to handle low impact tolerance

The previous parts of this article have illustrated a global behaviour of CMCs regarding impact, especially low velocity impact. Even if deeper investigations would allow to better understand the role of the material parameters (fibres and matrix nature, textile architecture, coating...) and the structure parameters (thickness, curvature, stiffness...), the sensitivity of CMCs to impact has been highlighted. A very explicit way to illustrate this fact is to simply consider the range of impact energies in which the impact regime thresholds are found. In most studies, they are located below 5 J and few take it up to 10 J. The comparison has to be made with any similar study on OMCs or with the ranges of impact energies indicated in the tests standards. These are roughly one order of magnitude superior to what was found here for CMCs. This sensitivity is common to all the CMCs regardless of their type of fibres, matrix or textile architecture. Consequently, it has to considered as an intrinsic behaviour of these materials for which little margin to improvement would be found.

The question raised in this final part is how to handle the low impact tolerance of CMC parts. With the previous postulate that no fully satisfying solution should be expected from the materials themselves, two axes are proposed here.

A first axis is to protect the CMC structural parts to prevent impact damages. Considering here the low velocity impact cases, it means establishing procedures to ensure as much as possible that a tool cannot be dropped on the part. Another way is to set up protective layers with shock absorbing materials, which could be placed during specific phases of the manufacturing and integration of part. The same solution may be applied to protect the sensitive parts of a system during its operational life, especially in the case of hail or pebble impact protection.

A second complementary axis is the inspection of sensitive parts to assess their structural health. The principle here is to ensure the reliability of the system, considering that a perfect protection may not be achieved. This requires to develop monitoring or in situ inspection devices that can be used by operators during the operational life of the system. IR thermography has been found to be a well-fitted method to investigate the impact damage in the previous results and in the reviewed studies. It could be a basis for such an inspection device since a portable system would not be very difficult to set up.

6. Conclusion

This study first investigated the damage behaviour of an oxide/oxide composite subjected to low velocity impact. The results have then been included in a database obtained from the literature involving impact tests on CMCs. Global trends have been identified. The impact velocity is the primary parameter that defines the damage behaviour. The sample thickness and stiffness also provide indications to assess the expected damage behaviour at a given incident energy.

The low impact tolerance of CMCs has been highlighted. Considerations on protection and detection were provided to try to counterbalance this weakness. The main point here is to take into account the expected specificity of use of systems involving these highly performant materials.

References

- V. Sodisetty, A. Singh, H. James, K. Lee et F. Benedict, «Damage evolution in quasi-1. statically indented alumina based oxide/oxide ceramic matrix composites: An experimental investigation,» Ceramics International, pp. 32491-32503, 48 (2022)
- 2. K. Ogi, T. Okabe, M. Takahashi, S. Yashiro, A. Yoshimura et T. Ogasawara, «Experimental characterization of high-speed impact damage behavior in a three-dimensionally woven SiC/SiC composite, » Composites Part A, pp. 489-498, (2010)
- D. Han, X. Jia, H. Zhang, X. Gao, X. Han, L. Sun, Z. Zhang, L. Zhang, F. Wang et Y. Song, 3. «Foreign object damage and post-impact tensile behavior of plain-woven SiC/SiC composites,» Composite Structures, 295 (2022)
- Y. Yang, F. Xu, Y. Zhang et G. Liu, «Experimental study on the impact resistance of 2D 4. plain-woven C/SiC composite, » Ceramics International, p. 15551–15559, 40 (2014)
- R. Bhatt, S. Choi, L. Cosgriff, D. Fox et K. Lee, «Impact resistance of uncoated SiC/SiC 5. composites,» Materials Science and Engineering A, pp. 20-28, 476 (2008)
- M. Presby, R. Mansour, M. Manigandan, G. Morscher, F. Abdi, C. Godline, A. Eftekharian et 6.

- S. Choi, «Characterization and simulation of foreign object damage in curved and flat SiC/SiC ceramic matrix composites,» Ceramics International, pp. 2635-2643, 45 (2019)
- 7. R. Olsson, «Mass criterion for wave control impact response of composite plates,» Composites: Part A, pp. 879-887, 31 (2000)
- 8. A. Singh, K. Kahle, H. James, A. Horner, D. Villaflor et Z. Benedict, «Environmental effects on the strength and impact damage resistance of alumina based oxide/oxide ceramic matrix composites,» Ceramics International, pp. 17268-17275, 47 (2021)
- 9. J. Thind, A. Singh, V. Tung, V. Le, W. Jackson, R. Meinders, T. Doan et B. Kitt, «Impact damage resistance and tolerance of alumina-based oxide/oxide ceramic matrix composite upon one sided thermal shock and hold,» J. Europ. Ceram. Soc., 44 (2024)
- 10. H. Mei, C. Yu, Y. Xu, D. Han et L. Cheng, «Effect of impact energy on damage resistance and mechanical property of C/SiC composites under low velocity impact,» Materials Science & Engineering A, pp. 141-147, 687 (1997)
- 11. C. Evci, «Thickness-dependent energy dissipation characteristics of laminated composites subjected to low velocity impact,» Composite Structures, pp. 508-521, 133 (2015)
- 12. S. Timoshenko et S. Woinowsky-Krieger, Theory of plates and shells, Mc Graw-Hill book compagny, (1959)
- 13. B. Liu, F. Li, Y. Liu et Y. Zhang, «Experimental and numerical studies on low-velocity impact of laminated C/SiC structures,» Composite Structures, 329 (2024)
- 14. L. Yao, P. Lyu, G. Bai et A. Augousti, «Influence of low velocity impact on oxidation performance of SiC coated C/SiC composites,» Ceramics International, p. 20470–20477, 45 (2019)
- 15. V. Herb, E. Martin et G. Couégnat, «Damage analysis of thin 3D-woven SiC/SiC composite under low velocity impact loading,» Composites: Part A, p. 247–253, 43 (2012)

Appendix: Data from the literature

Ref	Material		Sample dimensions (mm)			Impactor		Velocity	Energy (J)		Projected	Regime
	Туре	Modulus (GPa)	Thickness		Width	Ø (mm)	Mass (kg)	(m/s) [*]	Incident	Absorbed	damaged area (mm²)	_
	Ox/Ox	75		100	100	12.7			7.9 x10 ⁻²	3.1 x10 ⁻²	36	R
									9.5 x10 ⁻²	3.8 x10 ⁻²	56	R
									8.2 x10 ⁻²	3.0 x10 ⁻²	50	R
									0.2	0.11	112	R
									0.22	0.12	110	R
			2.5						0.19	0.1	114	R
									0.2	0.27	94	R
									0.4	0.25	120	R
[1]								2.1 x10 ⁻⁵	0.38	0.27	119	R
LTI									0.37	0.27	162	R
									0.7	0.56	138	R
									0.7	0.57	208	R
									0.6	0.52	208	R
									0.6	0.53	260	R
									0.96	0.85	247	R
									0.87	0.77	251	R
									0.93	0.83	226	R
									0.89	0.81	230	R
						1.5	1.4x10 ⁻⁵	1000	7.1			R
						2.5	6.4x10 ⁻⁵	467	6.8			R
[2]	SiC/SiC		6	33	33	2.5	6.4x10 ⁻⁵	805	20			Pen
						4	2.6x10 ⁻⁴	305	12			Pen
						2.5	6.4x10 ⁻⁵	900	25			Pen

HiSST: International Conference on High-Speed Vehicle Science Technology

Ref	Materia	ıl	Sample din	nensions	(mm)	Impact	or	Velocity	Energy (J)	Projected		Regime
	Туре	Modulus (GPa)	Thickness	Length	Width	Ø (mm)	Mass (kg)	(m/s)	Incident	Absorbed	damaged (mm²)	area	
								150	1.2		380		Pen
[2]	C:C/C:C	160	4	F0	20		1 1 10-4	200	2.2		380		Pen
[3]	SiC/SiC	162	4	50	20	3	1.1x10 ⁻⁴	250	3.4		32		Per
								350	6.8		54		Per
								79	1.6		54 25 30 44		R
						5		93	2.2		30		R R
)		99	2.5		44		R
								130	4.4				Pen
[4]	C/SiC		3	115	115			144	9.3		72		Pen
								147	9.7		85		Pen
						6		211	19.9		87		Per
								218	21.2		81		Per
								219	21.4		80		Per
								114	0.11		0.07		R
								160	0.21		23		R R R
								190	0.30		64		R
[5]	SiC/SiC	258	2.3	152	13	1.59	1.6x10 ⁻⁵	220	0.40		77		R
[2]	JIC/JIC	230	2.5	132	15	1.55	1.0×10	260	0.55		75		R
								300	0.73		75 52 58		R
								325	0.87		58		R
								375	1.15		75 43		R
					5.6			334	0.91		43		Pen
[6]	SiC/SiC	230	2.2	25.4	9.2	1.59	1.6x10 ⁻⁵	342	0.96		40		Pen
	•				12.7			341	0.96		27		Pen
											516		Pen
[8]	Ox/Ox	100	2.4	140	127	16	1.7x10 ⁻²	17.3	2.5		413		Pen
[[]	014 011										437		Pen
											1219		Pen
[9]	Ox/Ox	70	6.64	152	102	28	9.0x10 ⁻²	10.6	5		1148		Pen
											1012		Pen

Ref	Material		Sample dimensions (mm)			Impactor		Velocity	Energy (J)		Projected		Regime
	Туре	Modulus (GPa)	Thickness	Length	Width	Ø (mm)	Mass (kg)	(m/s)	Incident	Absorbed	damaged (mm²)	area	
								0.45	3		415		Pen
[40]	0/0/0	117		200	50	16	30	0.52	4		415		Pen
[10]	C/SiC		3					0.58	5		415		Pen
[13]								0.63	6		415		Per
									3				R
			3	80	70				5				Pen
									10				Pen
[13]	C/SiC	33							35	31.3			R
			17	150	100				57.7	54			R
									68.6	64.8			R
									67.5	65.3			R
	C/SiC	55	3	45	32	20		0.8	0.5				R
								1.1	1				R
[1 4]							1.67	1.5	2				R
[14]								1.9	3				Pen
								2.2	4				Pen
								2.4	5				Pen
							1.13	1.1	0.65	0.57			R
	SiC/SiC			24	24	9	1.13	1.5	1.31	1.26			R
			218 1.4				2.13	1.5	2.53	2.45			R
		218					2.13	2	4.3	3.9			Per
[15]							1.15	2	2.35	2.13			R
				150	100	12.7	1.15	2.1	2.46	1.85			R
							1.15	2.1	2.49	1.86			R
							1.15	1.6	1.47	1.09			R
							3.65	2.4	10.9	6.3			Per

HiSST: International Conference on High-Speed Vehicle Science Technology